

Model-based quantification of runoff generation processes at high spatial and temporal resolution

Andreas Steinbrich¹  · Hannes Leistert¹ · Markus Weiler¹

Received: 23 February 2016 / Accepted: 23 October 2016
© Springer-Verlag Berlin Heidelberg 2016

Abstract Heavy precipitation-induced flash floods are still a serious hazard and generate high damages. In the context of climate change, an increase of the occurrence of flash floods is very likely. To improve flash-flood predictions and allow measures to reduce damage in vulnerable catchments, the spatial dynamics of runoff generation at a high spatial resolution during extreme rainfall events need to be better predicted. The results of these models can then be included into hydraulic models to predict the surface water level and flow dynamics based on high-resolution topographic data. Long-term discharge data does generally not exist in the small headwaters mostly influenced by flash floods, which would allow to calibrate conventional rainfall-runoff models. But hydrological models predicting runoff generation processes without calibration based on available spatially distributed data sets are still lacking. Such a model [Runoff Generation Research (RoGeR)] was developed for the state of Baden-Württemberg. It is based on an extensive collection of spatial data, including a digital elevation model of $1 \times 1 \text{ m}^2$ resolution, degree of sealing of the earth surface for the same resolution, and soil properties and geology at the scale of 1:50,000. Within the state of Baden-Württemberg, different regions were selected encompassing distinct environmental characteristics regarding climate, soil properties, land use, topography

and geology. RoGeR was tested and validated by simulating 33 observed flood events in 13 mesoscale catchments without calibration and by modelling seven 60-m^2 artificial rainfall experiments on five different hillslopes in different regions of Switzerland. The results showed that the model was able to reproduce the temporal runoff dynamics as well as the peak discharge and the runoff volume in the mesoscale catchments as well as the 60-m^2 hillslope plots. The model could reproduce processes and hydrological response under different antecedent soil moisture and precipitation characteristics without any calibration, despite applying it to different regions and different scales. This suggests that RoGeR is predestinated to quantify runoff generation processes during heavy rainfall events at different scales without the typical model calibration procedure allowing to better quantify input and model uncertainty.

Keywords Runoff generation · Uncalibrated model · Infiltration · Preferential flow · Subsurface flow · Flash floods

Introduction

Streamflow gauging has been carried out in Germany and many other countries at many rivers for a long time. These streamflow time series are the basis for estimating return periods of floods and calibrating and applying rainfall-runoff models. Hence, flood hazards can be well predicted along most of the gauged rivers assuming unchanging catchment characteristics and climatic conditions. According to the EU Floods Directive, flood hazard maps along rivers have been generated for catchment areas larger than $10\text{--}20 \text{ km}^2$.

This article is part of a Topical Collection in Environmental Earth Sciences on “Water in Germany”, guest edited by Daniel Karthe, Peter Chiffard, Bernd Cyffka, Lucas Menzel, Heribert Nacken, Uta Raeder, Mario Sommerhäuser and Markus Weiler.

✉ Andreas Steinbrich
andreas.steinbrich@hydrology.uni-freiburg.de

¹ Hydrology, Faculty of Environment and Natural Resources, University Freiburg, Freiburg im Breisgau, Germany

Extreme rainstorms, especially in the summer, regularly lead to flash floods on hillslopes, in small watersheds, and in urban areas, often generating serious damage. In the context of climate change, it must be expected that the risk of extreme rainstorms will increase even further in central Europe (Berg et al. 2013). Due to the various difficulties in forecasting extreme rainstorms and measuring discharge in small catchments, there are virtually no long-term and continuous measurements of heavy rainfall-induced flash floods available. Hence, return periods for small-scale flash floods cannot be derived as is possible for larger watersheds. Furthermore, rainfall-runoff models which depend heavily on observed data cannot be calibrated (Beven 2011). However, to estimate the extent and magnitude of flash floods, it is crucial to estimate the spatial and temporal distribution of runoff generation during extreme precipitation without parameter calibration in a hydrological model and to represent the idiosyncrasies of individual hillslopes and headwaters.

In Germany rainfall-runoff models such as LARSIM (Bremicker 2000) or WaSIM-ETH (Schulla 1997) are widely applied and calibrated for catchments with measured streamflow data and therefore valid only for the scale of such catchments. For smaller sub-catchments or catchments without any streamflow gauges, the runoff generation processes might not be well represented. Moreover, many rainfall-runoff models do not take relevant infiltration processes through macropores and shrinkage cracks explicitly into account. Regionalization approaches to estimate runoff coefficients (e.g. US-SCS 1972; Lutz 1984) are only valid for mesoscale catchments and should be calibrated as well (DVWK 1984; Merz 2006). Furthermore, those simpler approaches only provide a constant runoff coefficient that does not consider the decrease of infiltration capacity during a rain event or the temporal rainfall characteristics. In addition, the contribution of fast subsurface flow on floods is not considered in such approaches. Markart et al. (2006) developed a method to estimate runoff coefficient classes for small alpine catchments considering a wide range of factors and processes. Since the method was developed for alpine catchments, it cannot easily be applied in other regions. Approaches to determine dominant runoff processes (e.g. LUWG 2006) identify the dominant runoff generation processes in high spatial resolution but do not specifically quantify the individual runoff amount, generated by that process.

Thus, so far, there is no rainfall-runoff model that is capable of quantifying runoff generation processes from the plot to the mesoscale in high spatial and temporal resolution without calibration while considering the relevant processes. Such a model should account for infiltration through macropores and shrinkage cracks as well as for fast subsurface flow through lateral preferential flow pathways. To fill

this research gap, the model RoGeR (**R**unoff **G**eneration **R**esearch) was developed at the University of Freiburg to quantify runoff generation in high spatial (up to $1 \times 1 \text{ m}^2$) and temporal (up to 5 min) resolution without the need to calibrate parameters. RoGeR combines the knowledge of runoff generation process research gained over the last decades with spatially distributed data sets describing vegetation and surface as well as subsurface properties. Since the model uses spatially distributed data containing all the information needed to describe the runoff generation processes at any place and any time, it can be applied to a wide range of spatial scales from the plot to mesoscale catchments without the need of a scaling factor. The suitability of RoGeR to properly quantify and predict runoff generation processes was validated on different scales using observed rainfall-runoff events and floods in a wide range of mesoscale catchments as well as with sprinkler experiments on larger hillslopes. This paper describes the considered processes, model architecture, and data requirements of RoGeR (“Runoff generation processes implemented into RoGeR” Section) as well as the model validation at different scales (“Validation of RoGeR” Section).

Runoff generation processes implemented into RoGeR

Overview

Figure 1 provides an overview of the processes relevant for runoff generation at the plot and hillslope scale, which have been implemented into RoGeR. Rainfall intensity and duration significantly influences the location, duration, and intensity of possible runoff generation processes (Weiler and Naef 2003). Generally, convective rainstorms with high intensity and usually short duration are more likely to produce Hortonian overland flow (HOF) due to infiltration excess. Long-duration advective events with low intensity typically produce saturation overland flow (SOF) and subsurface flow (SSF). The high intensities of convective storms often exceed the infiltration capacity of the soil matrix and can activate infiltration through macropore (Weiler and Naef 2003). However, the short duration and low amount is not sufficient to fill up the soil storage exceeding field capacity, which is a requirement for water release to deeper layers or the generation of subsurface flow. Advective events with low intensities rarely exceed the infiltration capacity of the soil matrix and only produce HOF on sealed or partly sealed surfaces.

The occurrence of HOF is required before infiltration through macropores (MP), and shrinkage cracks can occur. This infiltration through preferential flow pathways plays an important role in reducing HOF (Weiler and Flüßler 2004). Once field capacity is exceeded, water starts to

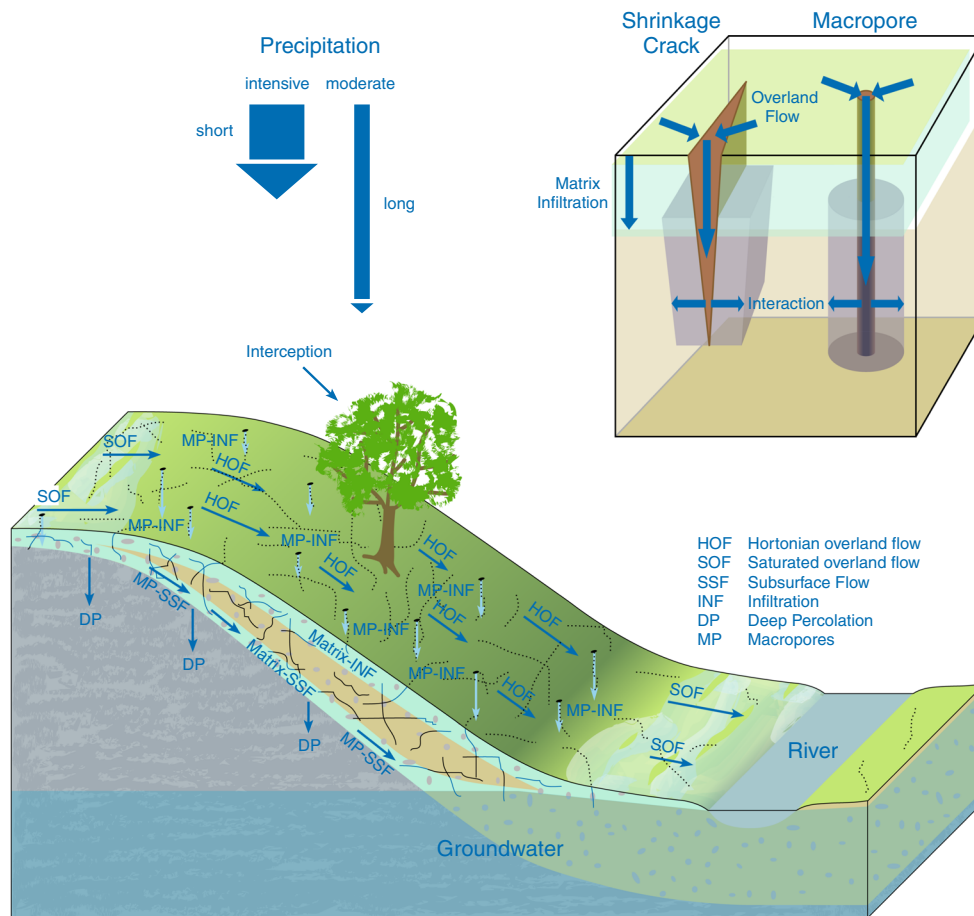


Fig. 1 Runoff generation processes implemented into the rainfall-runoff model RoGeR

percolate to the base of the soil. Depending on the permeability of the underlying material, water can continue to percolate vertically (deep percolation) or—if the amount of percolating water exceeds the capacity of the permeability of the material below the soil—a saturated zone develops at the base of the soil. From this saturated zone, subsurface flow (SSF) originates if the lateral permeability and gradient is large enough. SSF occurs as a slow component through the soil matrix and as a fast component through lateral preferential flow paths as, e.g. pipes or root channels (Scherrer 1997). When the soil becomes fully saturated, no more water can infiltrate and saturation overland flow (SOF) starts. This likely occurs especially in locations that have shallow soils with impermeable material below or in areas with a small distance to the groundwater table.

Interception and matrix infiltration

To quantify interception storage for single events, a leaf area index (LAI) approach was adopted including a seasonal dependence of the LAI into a simple interception storage model as described in Bremicker (2000). For sealed

or partly sealed areas, surface storage in microdepressions is quantified. Since RoGeR was designed as an event-based model, evaporation from interception storage is not considered.

For simulating infiltration into the soil matrix, the approach of Green and Ampt (1911), adjusted for time variable rainfall intensity by Peschke (1985), was implemented into RoGeR. The Green–Ampt approach assumes the formation of a uniformly saturated wetting front. Between the saturated and unsaturated soil, a suction head defined as the wetting front suction ψ is active. The infiltration velocity of the wetting front depends on the magnitude of the wetting front suction, the saturated hydraulic conductivity, the rainfall intensity and the unsaturated porosity, which is defined as the free plant available field capacity plus the free drainable porosity. The approach of Mein and Larson (1973) is implemented to estimate the wetting front suction ψ based on the water retention function.

$$\psi = \int_0^1 S dK_r \tag{1}$$

with S capillary suction and K_r relative unsaturated hydraulic conductivity (K/K_s).

K_r as a function of the capillary suction was estimated using a modified Mualem–van Genuchten (MvGM) model, accounting for an air entry value as described by Ippisch et al. (2006). The MvGM was parameterized for the 32 soil texture classes defined in a soil map available at a scale of 1:50,000 (BK50) for the state of Baden-Württemberg, Germany (Table 1) using the parameters recommended by Wessolek et al. (2009) for soils in Germany. The air entry value was set assuming a maximum pore diameter of 5 mm related to a pressure head of 0.58 cm. The soil map BK50 also distinguishes between different soil horizons. The plant available field capacity, the drainable porosity and saturated hydraulic conductivity are explicitly parameterized in the digital map for agricultural and non-agricultural land use. The antecedent soil moisture and thus the free porosity at the beginning of events is derived from the output of the model GWN-

BW (Groundwater recharge model for Baden-Württemberg; Gudera and Morhard 2015). Daily soil moisture data from the GWN-BW model is available since 1971 for the entire area of Baden-Württemberg. During the running of the model, RoGeR computes the potential matrix infiltration and the depth of the wetting front for each time step and cell. The potential matrix infiltration is reduced to the actual matrix infiltration by the degree of sealing of the surface. Finally precipitation minus interception minus actual matrix infiltration results in the potential HOF.

Infiltration through macropores and shrinkage cracks

The soil matrix properties are not sufficient to predict runoff response to heavy rainfall. For example, Scherrer (1997) was able to show in numerous sprinkler experiments with high rainfall intensities on larger hillslopes that,

Table 1 Database and use in the model currently available for Baden-Württemberg

Data set	Resolution/scale	Data provider	Use in model
ATKIS DLM25	1:25,000	Landesvermessungsamt Baden-Württemberg (LV-BW)	Parameterization of macropores, interception and wetlands
CORINE land cover 2000	Min. polygon size $500 \times 500 \text{ m}^2$ min. line width 100 m	Umweltbundesamt, Berlin	Parameterization of macropores, interception and wetlands
Degree of sealing of earth surface	$1 \times 1 \text{ m}^2$ -grid	Wasser- und Bodenatlas Baden-Württemberg (WaBoA)	Reduction of infiltration
LIDAR data	$\sim 1 \times 1 \text{ m}^2$	LV-BW	Digital elevation model (DEM), vegetation height, slope, flow accumulation, depth to groundwater
River network as line file	1:10,000	Landesanstalt für Umwelt, Messung und Naturschutz Baden-Württemberg (LUBW)	Ideal to define a river network from the DEM
Lakes as polygon file	1:10,000		Open water
Soil overview map of Baden-Württemberg (BÜK)	1:200,000	Regierungspräsidium Freiburg Landesamt für Geologie, Rohstoffe und Bergbau (LGRB)	Soil storage, soil depth, portion of skeleton, soil texture classes
Soil map 50,000 (BK50) (available since 2015/6)	1:50,000		Soil storage, soil depth, portion of skeleton, soil texture classes, saturated hydraulic conductivity
Hydrogeological map	1:50,000		Transmissibility of under laying material and bedrock
Precipitation radar data for selected events (RADOLAN)	$\sim 1 \times 1 \text{ km}^2$ 1 h-sum	Deutscher Wetterdienst (DWD)	Input for modelling selected flood events
Precipitation data from gauging stations	5-min sum	DWD	Control and evaluation of precipitation radar data
GWN-BW (groundwater recharge in Baden-Württemberg)	Daily average soil moisture, average area 0.8 km^2	LUBW	Estimation of spatial antecedent soil moisture conditions
Discharge data from gauging stations	1-h averages	LUBW	Evaluation of modelled discharge at gauging station

frequently, more water can infiltrate than expected because of the soil matrix properties. Infiltration through preferential flow paths like macropores (i.e. earthworm channels) or soil cracks is cited as the reason of this phenomenon, which is playing an important role in runoff generation during high rainfall intensities (e.g. Beven and Clarke 1986; Weiler 2001, 2005; Weiler and Naef 2003; Weiler and Flühler 2004). Consequently, the macropore infiltration process is implemented in RoGeR. Ponding water, described as potential Hortonian overland flow, is a prerequisite for infiltration through preferential flow paths. However, only a certain proportion of overland flow is connected to macropores. The magnitude of this proportion is related to the macropore density (Weiler and Flühler 2004). The other part of the overland flow cannot infiltrate via macropores and hence will run off. How much water actually infiltrates via macropores depends on the interaction between macropores and soil matrix. This horizontal infiltration from the macropores into the soil matrix is estimated using the Green & Ampt method, which needs to be modified for horizontal direction with a radial wetting front for this purpose (Beven and Clarke 1986; Weiler 2005; Fig. 1, top right). During the infiltration process, the progressing wetting front of vertical matrix infiltration from the soil surface successively shortens the active part of the macropore (Fig. 1, top right).

To model macropore infiltration, it is crucial to estimate the macropore density, length and diameter. Activities of soil animals, in particular *Lumbricus terrestris* (common earthworm), root penetration and soil processes in connection with climate conditions (e.g. expansion/shrinking of clay), are expected to be the first-order controls of macropore formation (Casper 2002; LUWG 2006). It is not well investigated yet to what extent which processes are actually involved in the formation of macropores at a specific site (LUBW 1997; Schmocker-Fackel 2004). Investigations related to macropore properties of soils

suggest a high heterogeneity in space and time even under similar environmental conditions (Schmocker-Fackel 2004). Thus, more investigations are urgently needed to predict the spatial and temporal macropore properties using environmental data as predictors. Vertical as well as lateral macropores, which are relevant for fast subsurface flow (Fig. 1), were parameterized based on different factors found in the scientific literature (LUBW1997; Jarvis et al. 2009; Lindahl et al. 2009; Van Schaik 2009; Geitner et al. 2014). A relation between the length of macropores and land use was assumed in the model (Table 2). In forests, the density of macropores is expected to be particularly high as the result of undisturbed bioactivity and root penetration. Since the most common coniferous tree species in the state of Baden-Württemberg, spruce (*Picea abies*), are shallow rooting (Raissi et al. 2009), a reduced length of vertical macropores was defined for coniferous forests compared to deciduous forests. In crop land and vineyards, vertical macropores tend to be disturbed as a consequence of the frequent soil treatment of these sites (Winter 2013). This effect is reflected in the model through a reduced density of vertical macropores for these land cover types. The discordance of the plough layer is considered by a reduction of the length of vertical macropores for crop land. In relation to the skeleton content in the soil, which generally enhances preferential flow (Moldenhauer et al. 2013; Sohrt et al. 2014), the density of macropores was increased by 25 m⁻² for skeleton contents between 10 and 25% and by 50 m⁻² for skeleton contents between 25 and 50%. All macropores (vertical and lateral) are parameterized with a diameter of 5 mm, corresponding to a cross-sectional area of 20 mm². The selected macropore parameters shown in Table 2 lie within plausible limits found in literature.

In particular for clay soils, shrinkage cracks occur during dry periods. Like macropores shrinkage cracks can contribute substantially to the infiltration process (e.g.

Table 2 Estimation of macropore density and length for land cover classes and *k* values for overland flow (vertical macropores for infiltration process, slope parallel macropores for subsurface flow)

Land cover class	Density of vertical macropores (MP/m ²)	Length of vertical macropores (cm)	Density of slope parallel macropores (MP/m ²)	Strickler <i>k</i> values for overland flow
Settlement (1–100% sealed)	75–0	30	125	75
Crop land	75	30	125	30
Pasture	100	80	125	20
Wine yards	75	50	125	30
Orchard	100	50	125	20
Garden	100	30	125	25
Deciduous forest	150	50	150	20
Mixed forest	150	50	150	20
Coniferous forest	150	30	150	30
Wetlands	0	0	0	100

Baram et al. 2012). The depth of shrinkage cracks depends on the clay content and the soil water content. Between the soil moisture content at which the process of cracking starts and the soil moisture content at which no further volume decrease of the soil occurs, RoGeR assumes a linear temporal evolution of cracks. The soil moisture content at which compact soils are no longer plastically formable is set as the starting value for the formation of shrinkage cracks. The matrix potential related to this soil moisture content is defined by a value of 500 hPa (Ad hoc-Arbeitsgruppe Boden 2005). The end of the crack development process is defined by the shrinkage limit value related to a soil matrix potential of 10,000 hPa (Ad hoc-Arbeitsgruppe Boden 2005). At this soil moisture, cracks reach their maximum depth. By applying the Mualem–van Genuchten model to the texture classes of the soil map 1:50,000 (Table 1), again using the parameterization after Wessolek et al. (2009), the fraction of saturated pore volume of the entire pore volume can be estimated for any given matrix potential. For known antecedent moisture content, the depth of shrinkage cracks can then be estimated by:

$$z_c = (C - C_{\min}) * F * \left[1 - \frac{(\theta_{\text{akt}} - \theta_{\text{sl}})}{(\theta_{\text{pl}} - \theta_{\text{sl}})} \right] \quad \text{for } \theta_{\text{akt}} < (\theta_{\text{pl}} \text{ and } \theta_{\text{act}}) \theta_{\text{sl}}$$

$$z_c = 0 \quad \text{for } \theta_{\text{akt}} \geq \theta_{\text{pl}}$$

$$z_c = (C - C_{\min}) * F \quad \text{for } \theta_{\text{akt}} \leq \theta_{\text{sl}}$$
(2)

with z_c depth of the shrinkage crack (mm), θ_{pl} water content at matrix potential of 500 hPa (begin or crack formation), θ_{sl} water content at matrix potential of 10,000 hPa (shrinkage limit), θ_{akt} actual Water content [-] C percentage of clay, C_{\min} minimum percentage of clay and F increment of increase of crack depth (mm) per 1% of increase of clay content.

C_{\min} is set to 3% and F to 7 mm so that the depth of the cracks at the shrinkage limit (maximum depth) equals 500 mm for the soil with the highest clay content (75%). This value lies within the range found in literature (e.g. Baram et al. 2012) and own field studies. Shrinkage cracks typically build a more or less polygon-shaped network (e.g. Baram et al. 2012). According to different studies (Bouma and Dekker 1978; Konrad and Ayad 1997; Li and Zhang 2010; Baram et al. 2012) and own field observations on pelosols around Freiburg (Baden-Württemberg), an average distance between cracks of 20 cm was set resulting in a crack density of 10 m/m².

The horizontal infiltration process from the shrinkage cracks into the soil matrix is simulated with the Green–Ampt assumption considering a linear progressing wetting front from both sides of the crack. Based on Darcy’s law, the progress of the wetting front can be formulated by:

$$\frac{dx}{dt} = k_s \left(\frac{\psi}{x \Delta \theta} \right)$$

$$t = \frac{x^2 \Delta \theta}{2 k_s \psi}$$

$$x(t) = \sqrt{\frac{2 k_s \psi t}{\Delta \theta}}$$
(3)

with x horizontal distance between wetting front and the wall of the crack (m), k_s saturated hydraulic conductivity (m/s), ψ wetting front suction (m), $\Delta \theta$ change of water content at the wetting front (-) and t time (s).

From this, the potential infiltration form shrinkage cracks can be derived:

$$I_{\text{pot}}(t) = 2 z_c D_c \Delta \theta \frac{(x(t) - x(t - \Delta t))}{\Delta t}$$
(4)

with I_{pot} potential infiltration (m/s), z_c depth of shrinkage cracks (m) and D_c crack density (m/m²). As described for macropores, the progressing vertical wetting front of the infiltration from the soil surface successively shortens the active length (z_c) of the cracks.

Soil storage, deep percolation, subsurface flow and saturation overland flow

Potential soil storage at the beginning of a rainfall event is given by the free proportion of the available field capacity plus the free drainable pore volume. Infiltration through matrix and preferential flow paths fills this soil storage. If the available field capacity is exceeded, water is percolating deeper (field capacity excess). The potential deep percolation flux into the underlying geological substrate is derived from the hydrogeological map (Table 1). If more water percolates out of the soil than the bedrock can absorb, this water (deep percolation excess) starts to fill up drainable pore volume from the base of the soil. Consequently, a saturated layer develops, which represents the active zone for subsurface flow through the soil matrix and lateral macropores. The deep percolation excess is also the amount of water available for subsurface flow.

RoGeR divides the subsurface flow into a slow and a fast component. The maximum lateral flow by slow subsurface flow through the soil matrix is estimated using Darcy’s law for flow in saturated conditions. The maximum lateral flow by fast subsurface flow through preferential flow pathways is expected to depend on the lateral macropore density, connectivity and slope (Weiler and McDonnell 2004). Both, density and connectivity are expected to decrease with depth as a consequence of increasing bulk density, decreasing root density and decreasing activity of soil animals with depth. Hence, flow velocity and amount are expected to be smaller for deep subsurface flow compared to shallow subsurface flow.

There are no sufficiently comprehensive data sets or empirical relations available to prove this assumption. Such a data set should be based on field experiments and should include flow velocities of SSF as well as properties like depth of the flow process, antecedent soil moisture, slope, land cover and slope length as all these factors might influence flow velocity. However, only a couple of data sets could be found that relate lateral flow velocity to slope and depth in the soil (Fig. 2). The number of experiments with additional information about the depth of the processes (number 1, 2, 3 and 6 in Fig. 2) is not sufficient to prove a significant relationship between depth of subsurface flow and flow velocity. However, a tendency that supports the hypothesis of decreasing flow velocity with depth is evident. Finally, eight relationships were derived between flow velocity and slope for different depth classes where the fast subsurface flow occurs (=saturated layer). These relationships reflect the range of observed flow velocities reported in literature. Kohl et al. (2012), for example, reported flow velocities of fast SSF ranging from 0.3 to 180 m/h. By applying the relationship shown in Fig. 2, the maximum flow capacity for subsurface flow through macropores can be calculated for each grid cell:

$$SSF_{MPpot} = \sum_{k=1}^8 z_{sat}(H_k) v_k(i) d_h A_{MP} \tag{5}$$

with $SSF_{MP\ pot}$ maximum possible SSF flow through lateral macropores (m^3/h), i slope (m/m), H_k horizon k , $z_{sat}(H_k)$ saturated thickness of the k th horizon (m), $v_k(i)$ slope dependent velocity in the k th horizon (m/h), d_h density of slope parallel macropores (MP/m^2) and A_{MP} cross-sectional area of one macropore (m^2).

Water, available for subsurface flow (deep percolation excess), is allocated to (slow) matrix subsurface flow and (fast) macropore subsurface flow according to the quantitative relation between the potential maximum SSF flow of matrix and MP. If the amount of infiltrated water still exceeds the soil porosity after losses by deep percolation and SSF are considered, saturation overland flow is generated by saturation excess. In areas with a high groundwater table, the total available storage of the soil is reduced by the groundwater. An average initial groundwater table is estimated applying the GIS method “vertical distance to groundwater”, available with the GIS software SAGA (Olaya 2004).

Flow accumulation

In a first step, RoGeR was developed to quantify the spatial and temporal runoff generation processes. Since runoff generation is commonly not measured, one way to test the model is to route the individual flow components

Table 3 Model parameter (per grid cell)

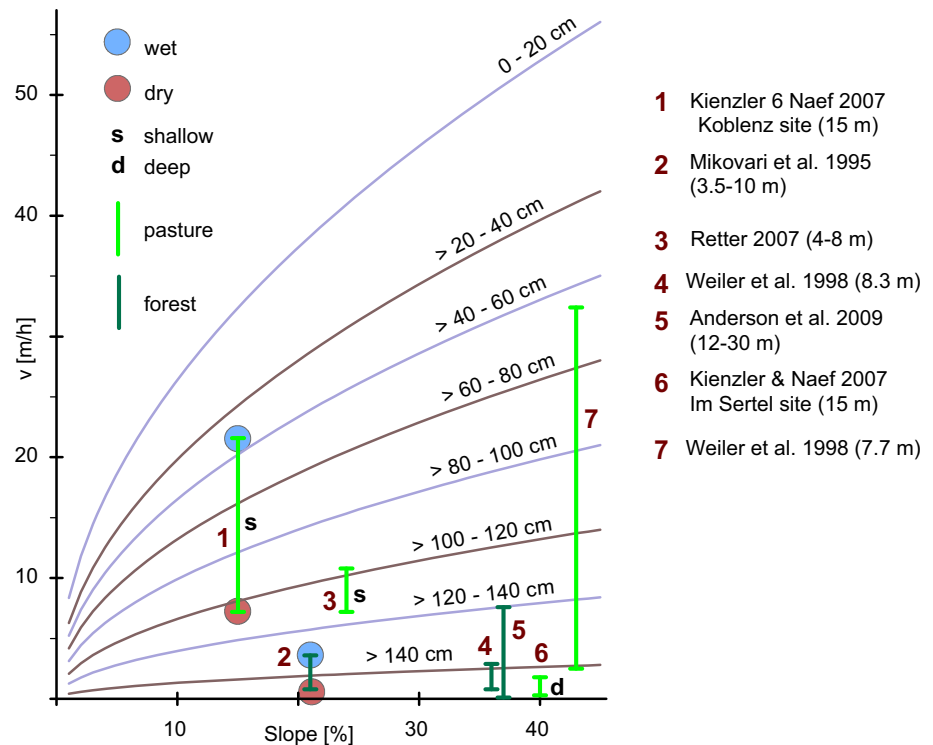
Model parameter	Unit
Event independent	
Land use	(-)
Degree of sealing	(-)
Surface slope	(-)
Density of vertical macropores	(L ⁻²)
Depth of vertical macropores	(L)
Density of slope parallel macropores	(L ⁻²)
Mean distance of shrinkage cracks	(L)
Depth of groundwater level	(L)
Soil depth	(L)
Plant available field capacity of soil	(-)
Air capacity of soil	(-)
Saturated hydraulic conductivity of soil	(L T ⁻¹)
Wetting front suction	(L)
Saturated hydraulic conductivity below the soil	(L T ⁻¹)
Velocity of overland flow	(L T ⁻¹)
Velocity of fast (preferential) subsurface flow	(L T ⁻¹)
Velocity of slow (matrix) subsurface flow	(L T ⁻¹)
Velocity of groundwater	(L T ⁻¹)
Event dependent	
Interception storage	(L)
Free plant available field capacity	(-)
Free air capacity	(-)
Depth of shrinkage cracks	(L)
Time step dependent	
Precipitation	(L T ⁻¹)

to a stream gauging station and to compare modelled and measured hydrographs. For this purpose, routing routines were implemented into the model. For the different flow components (overland flow, fast subsurface flow, slow subsurface flow and groundwater flow), separate geomorphic unit hydrographs are calculated using common GIS methods. The classification of flow accumulation is set to reproduce the river network 1:10,000 (Table 1). Overland flow is assumed as sheet flow with a depth of 1 mm. The Manning–Strickler equation is applied using Strickler k values in dependence of land cover (Table 3). For flow in rivers, a uniform velocity of 3 m/s is assumed implying high streamflow velocities during floods. Flow velocities of fast subsurface flow via macropores are estimated by:

$$V_{SSF} = \frac{\sum_{k=1}^8 dth_{sat}(H_k) \times v_k(i)}{\sum_{k=1}^8 dth_{sat}(H_k)} \tag{6}$$

with: V_{SSF} mean velocity over macropores (m/h), i slope (m/m), H_k horizon k , $dth_{sat}(H_k)$ saturated thickness of the k th horizon (m) and $v_k(i)$ slope dependent velocity in the k th horizon (m/h) (see also Fig. 2).

Fig. 2 Flow velocity of fast subsurface flow. The *curved lines* define the relationship between slope and mean flow velocity for 8 depth classes of soil in the model. The *vertical straight lines* represent the range of observed velocities of different field experiments at one or more hillslope sections. *Colours of vertical lines* show the land cover type. Additional information is shown in the legend



In areas with karst phenomena, water percolating into the limestone rock might also contribute to the hydrographs of flood events. Therefore, flow velocity in karstic aquifers had to be estimated. A uniform velocity of 0.012 m/s was set for groundwater flow in karst systems (Pohl 2000). This simple approach proved to be appropriate to correctly model secondary discharge peaks that were observed for two flood events in catchments with considerable karst influence. Figure 3 shows the spatial distribution of flow times to the gauging station for surface and fast subsurface flow in the Brugga catchment (No. 11 in Fig. 6). It was found that the shape of hydrographs for mesoscale catchments were well represented by the implemented geomorphic unit hydrograph approach for different flow components. This highlights the relevance of the spatial distribution of runoff generation and flow times for the shape of hydrographs. For small areas and high rain intensities, in particular in residential areas, a dynamic hydraulic 2D approach might be more appropriate than a static unit hydrograph approach. High flow concentration on roads might lead to much higher flow velocities than the assumed sheet flow with a depth of 1 mm. A dynamic hydraulic 2D approach therefore is currently implemented into RoGeR.

Database

The increasing availability of high-quality, spatially distributed geodata allows the application of the spatially

distributed model RoGeR. RoGeR was first developed for use in the state of Baden-Württemberg (BW) in the southwest of Germany and set up with spatial data sets (Table 1) available for the entire area of BW. But any appropriate spatial data sets can be used to estimate the required parameters of RoGeR (Table 3). This means that improved input data can replace currently used data or that the model can easily be transferred to other study areas. The spatial resolution of the actual available data varies between $1 \times 1 \text{ m}^2$ (e.g. degree of sealing, topography) and $1 \times 1 \text{ km}^2$ (rainfall radar data). Using particular preprocessing modules implemented in RoGeR, required raster data sets of the model parameters can be derived from the various input data sets and formats. The land use information of CORINE, available in comparatively low resolution, is supplemented by information on the river network extracted from the DEM, the degree of sealing of the earth surface, and the information about the height and location of trees and bushes, extracted from a BW wide LIDAR data set (Fig. 4). Data sets of event independent parameters (see Table 3) have been generated for the entire area of BW ($\sim 36,000 \text{ km}^2$) with a resolution of $5 \times 5 \text{ m}^2$ and for 13 mesoscale test catchments with a resolution of $1 \times 1 \text{ m}^2$. The event dependent parameters are generated based on long-term water balance simulation [e.g. GWN-BW (Groundwater recharge model for Baden-Württemberg; Gudera and Morhard 2015)] or other pre-defined definitions.

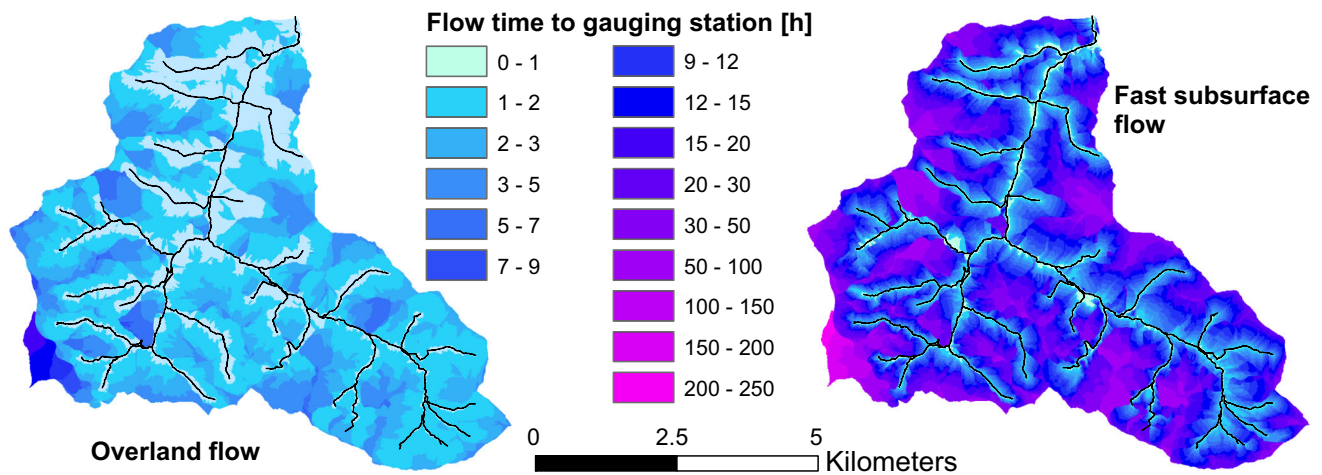


Fig. 3 Flow times for overland flow and fast subsurface flow in the catchment of the gauging station Oberried/Brugga (no.11 in Fig. 6)

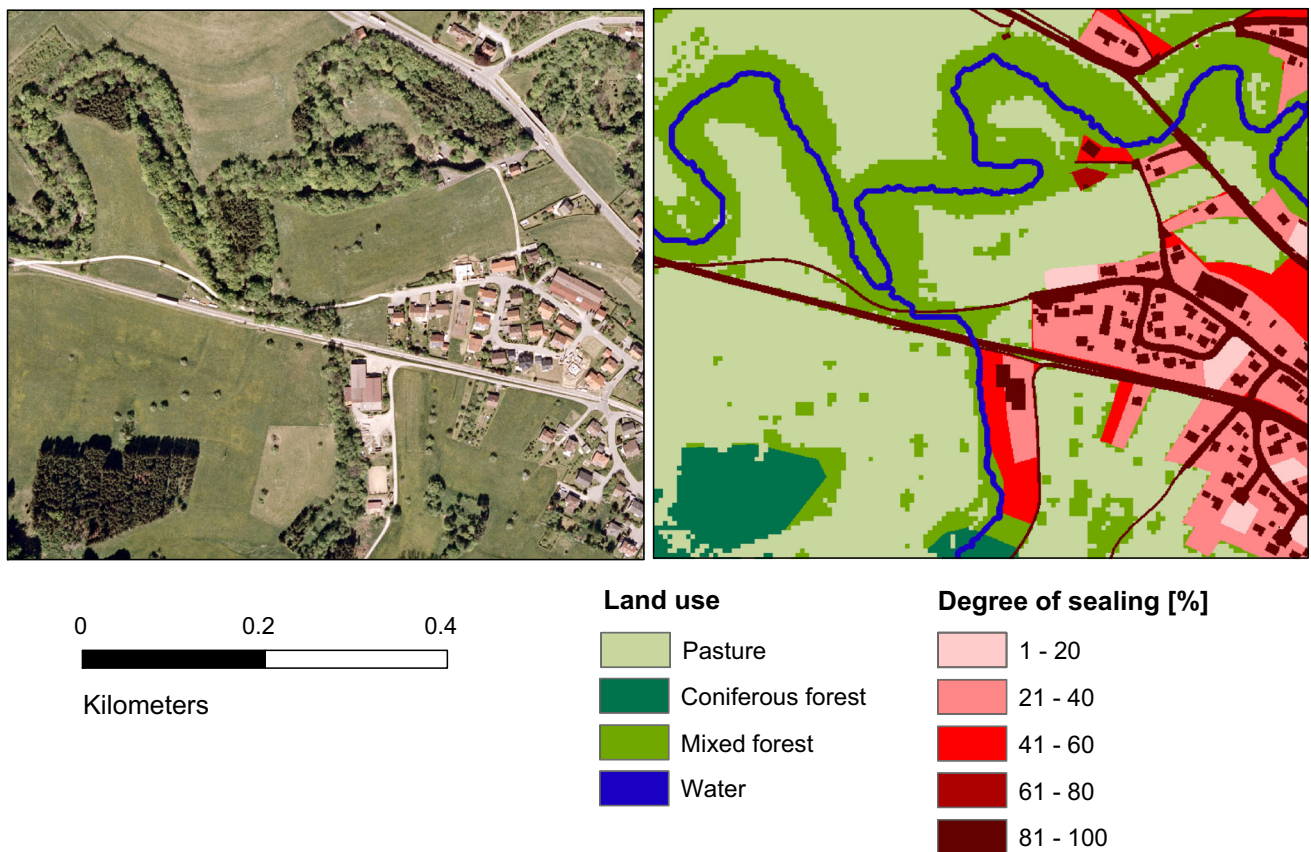


Fig. 4 Combination of land use information from different sources to derive a composed database for RoGeR (left side air photograph for comparison, right side model input at a spatial resolution of $1 \times 1 \text{ m}^2$)

Validation of RoGeR

RoGeR’s capability to correctly reproduce runoff generation process and the resulting discharge reaction was validated for two different spatial scales. At the hillslope scale, sprinkler experiments with measurements of

overland flow and subsurface flow were used to directly compare the simulated runoff generation processes. At the mesoscale, observed flood events in catchments with gauging stations were modelled with RoGeR and the model simulations were compared to the observed streamflow hydrographs.

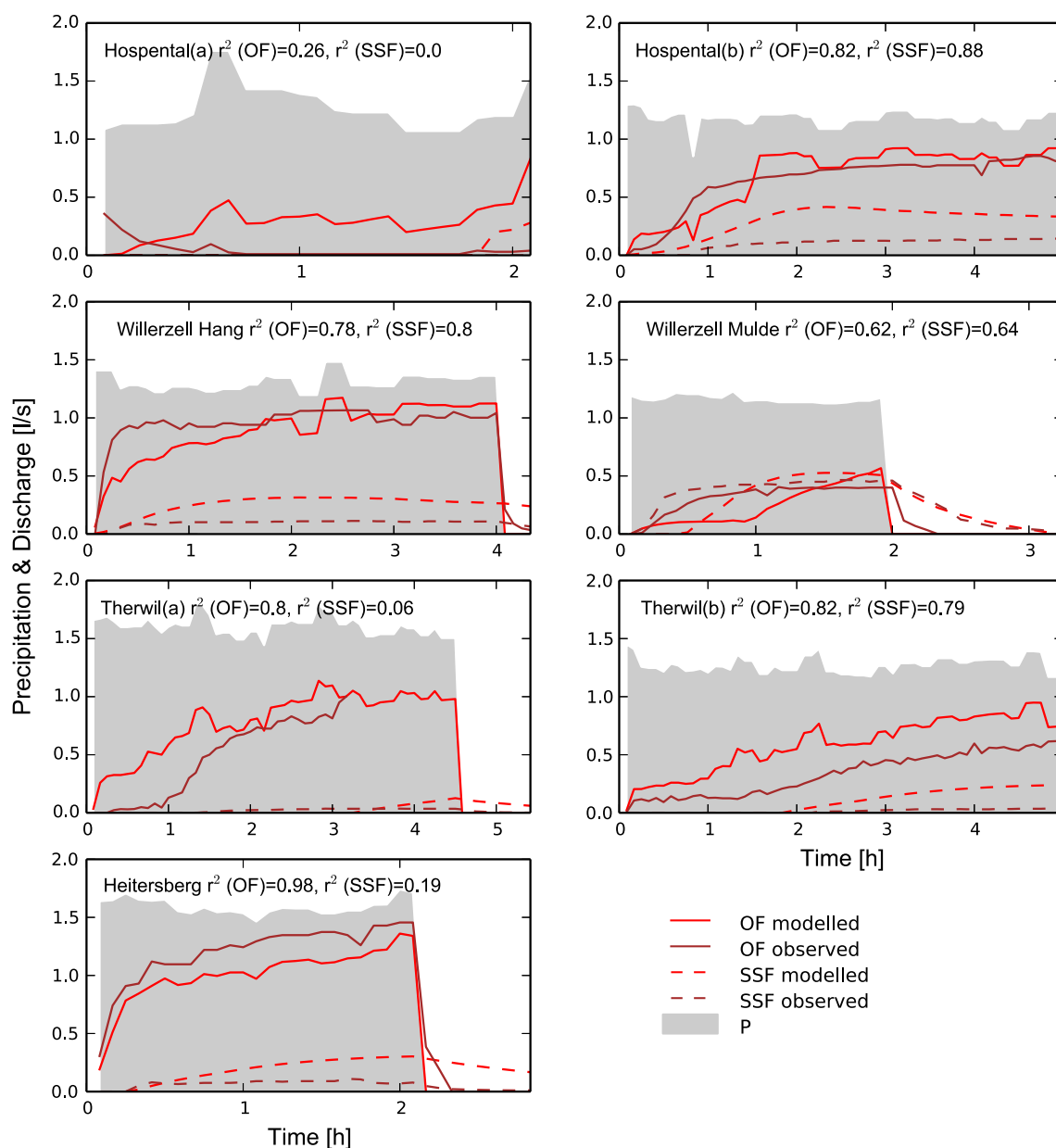


Fig. 5 Measured and modelled runoff components of sprinkler experiments in four different regions of Switzerland. The two experiments represented in the *upper* and *third* row are from the same slope under dry conditions (*left*) and more wet conditions

(*right*). The two experiments in the second row are from neighbouring slopes. One at mid slope (*left*) and one at the toe slope (*right*). *OF* overland flow, *SSF* subsurface flow and *P* precipitation

Sprinkler experiments

Sprinkler experiments at hillslopes provide the opportunity to measure runoff generation processes separately for overland flow and subsurface flow under controlled conditions. To avoid the influence of boundary effects, the sprinkled area should be as large as possible. Scherrer (1997) performed sprinkler experiments on an area of 60 m² with high rainfall intensities (50–100 mm/h) on 18 slopes in different regions of Switzerland. Runoff data as well as data about soil properties, antecedent soil moisture,

land use and the geological underground from seven experiments were used to set up the model RoGeR in order to test its ability to reproduce the results of the runoff measurements during the experiments. RoGeR was parameterized with the available soil property data and not calibrated. Figure 5 shows the result of the simulations. Only one experiment could not be modelled with satisfying results (upper left in Fig. 5). A hydrophobic reaction of the dry soil surface played a major role in this case (Scherrer 1997). This process is not implemented in RoGeR. The sprinkler experiment represented by the upper right graph

in Fig. 5 was conducted at the same plot under wetter conditions without hydrophobic influences. In this case, as well as in the other five experiments, the dynamics of overland flow as well as subsurface flow was well reproduced. It is particularly notable that the quantitative relation between the different flow components was well represented. A slight overestimation of the measured subsurface flow was found in all model runs. This might be explained by the challenge to capture all subsurface flow during the field experiments (Scherrer 1997).

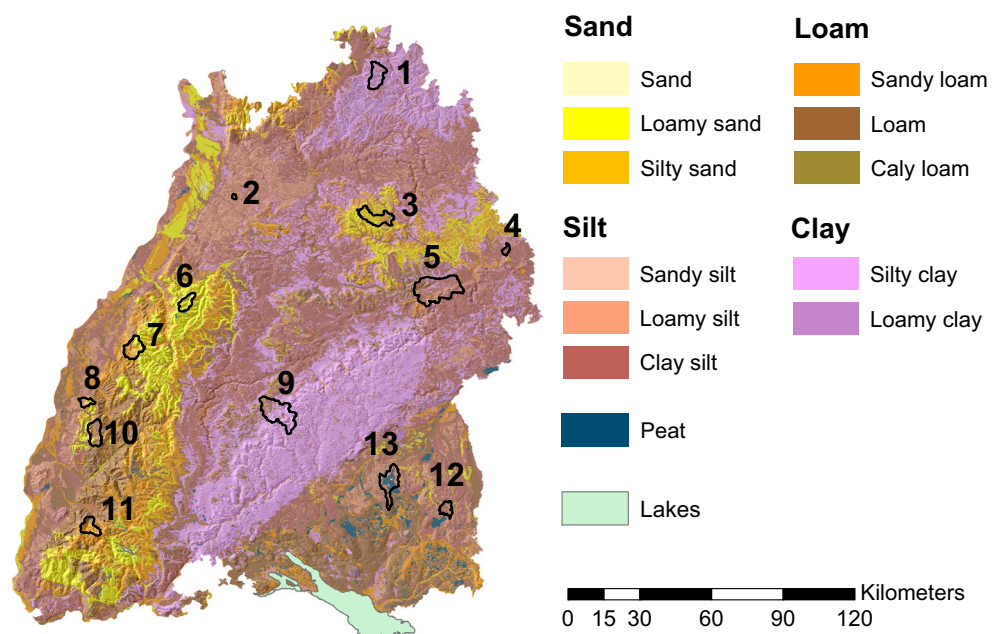
Mesoscale catchments

Runoff generation in space and time is usually not measured during natural rain events. The only information available is the integrative streamflow response of the catchment at a gauging station. The shape of the hydrograph depends considerably on the temporal and spatial distributions of the runoff generation processes (e.g. McGlynn et al. 2004; Zillgens et al. 2007). Events dominated by overland flow processes generally show a fast increase and fast decrease of the hydrograph as well as relatively high peak discharge but small runoff yields. In contrast, events with dominating subsurface flow generate hydrographs of moderate peak flow but long-lasting recession and large runoff yield. Thus, besides the peak discharge and runoff coefficient, the shape of the hydrograph is a suitable indicator to verify the ability of a model to correctly reproduce the processes of runoff generation.

RoGeR was used to simulate 33 flood events in 13 mesoscale catchments within the state of Baden-Württemberg (BW; Fig. 6). The catchments represent almost the

entire range of land uses, soils and geology occurring in BW. The simulated events also cover different rainfall event types (advective and convective) and a wide range of antecedent moisture conditions. Similar to the simulation of runoff at the hillslopes, the model parameters were not calibrated but set as described in the method section. Figure 7 shows exemplarily the simulation results for three short convective rain events (left side) and three longer advective events (right side) in comparison with the observed streamflow in three catchments with different soil characteristics. Catchment no. 9 is dominated by clay soils, no. 10 by loamy soils and no. 6 by sandy soils. Note that for the short convective rain events 5-min sums of precipitation are displayed, while for the longer advective events 1-h sums are shown, which are also the time steps used in the model for the respective events. With one exception (lower row), the convective rain events led to a fast discharge rise with high peak discharge and a fast recession. For catchments no. 9 (Starzel) and 10 (Schutter), the observed hydrographs, which were dominated by Hortonian overland flow (HOF), were well represented by the simulations. In the case of catchment no. 6 (Eyach), HOF and saturation overland flow (SOF) were overestimated by the model. This is surprising, since HOF was only generated on forest roads in this catchment dominated by forest cover. In reality, HOF might have re-infiltrated into the sandy soils after leaving the roads. This process cannot be simulated by the approach of a static geomorphic unit hydrograph approach. Saturation overland flow was generated in areas along the rivers that cover about 1.5% of the catchment area. A similar value was also published by Casper (2002) for this watershed and is hence in line with

Fig. 6 Location of mesoscale catchments in Baden-Württemberg used for verifying the RoGeR model. The catchment numbers are the same as used in Figs. 7 and 8



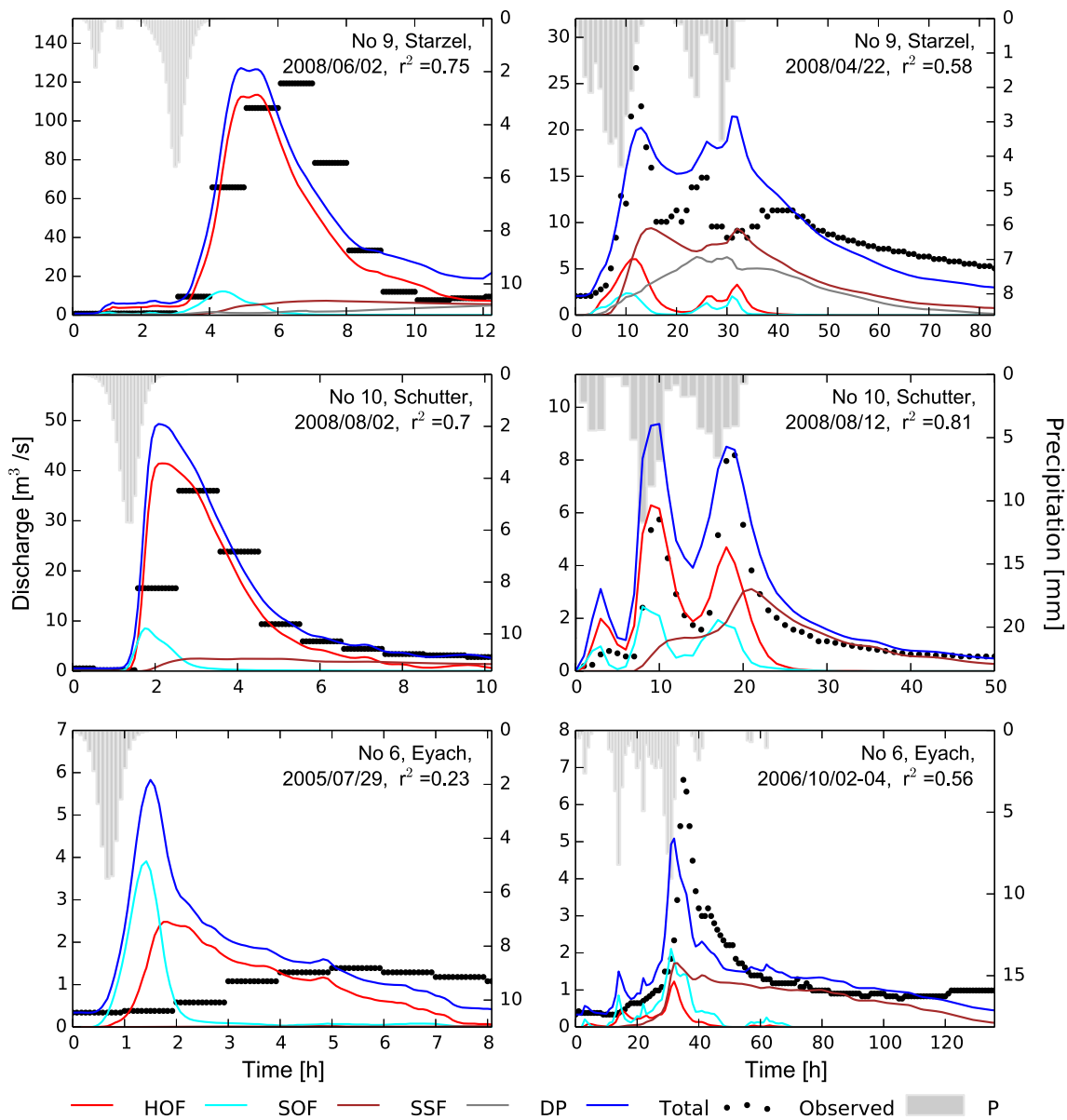


Fig. 7 Model results for six events in three different mesoscale catchments. Catchment no. 9 (*upper row*) is dominated by clay soils, no. 10 (*middle row*) by loamy soils and no. 6 (*lower row*) by sandy soils. The rain events on the *left* side are of short convective type, and thus, the model was applied in 5-min steps. Note that precipitation

bars represents 5-min sums in this case. On the *right* side long-lasting advective rain events are modelled in hourly time steps. Precipitation bars represents 1-h sums. *HOF* Hortonian overland flow, *SOF* saturation overland flow, *SSF* subsurface flow, *DP* deep percolation, *P* precipitation

the simulations. The groundwater table and, as a consequence, the area producing SOF within RoGeR is estimated using information of river network and topography (see chapter 2.4). There is no variation with differing initial wetness condition implemented yet. Thus, the groundwater level might have been estimated too high for the relatively dry conditions at the time of this event (see Fig. 8).

The long-lasting advective events are characterized by moderate peak discharges and long-lasting recessions. Both were well reproduced by RoGeR. Fast subsurface flow (Fig. 7, brown line) is the major process responsible for the

long recession in all catchments. In catchment no. 9 (Starzel), the outflow from Karst springs contributes to those events as well, which is reflected by the predicted deep percolation runoff (grey line) within RoGeR. Usually, the contribution of this flow component to the flood hydrograph predicted by RoGeR is marginal. But based on typical flow velocity in Karst systems, it is assumed that this runoff component will contribute significantly to the event runoff for catchments located in limestone areas.

An overview of the results for all catchments and events is given in Figs. 8 and 9. Figure 8 shows the process

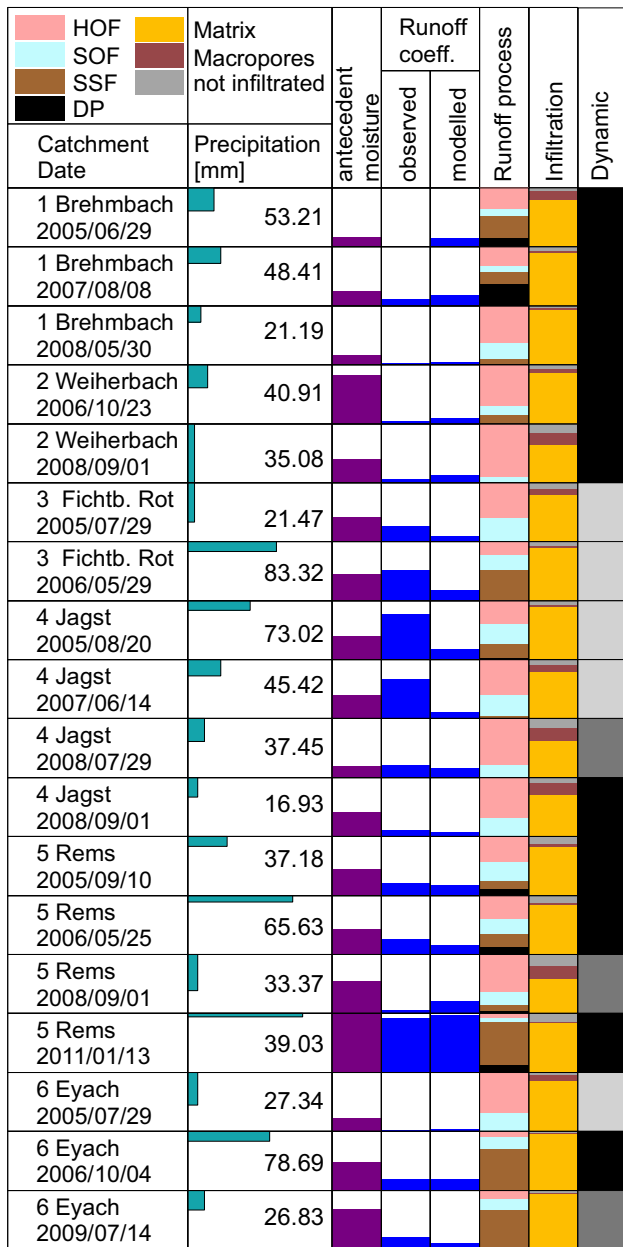
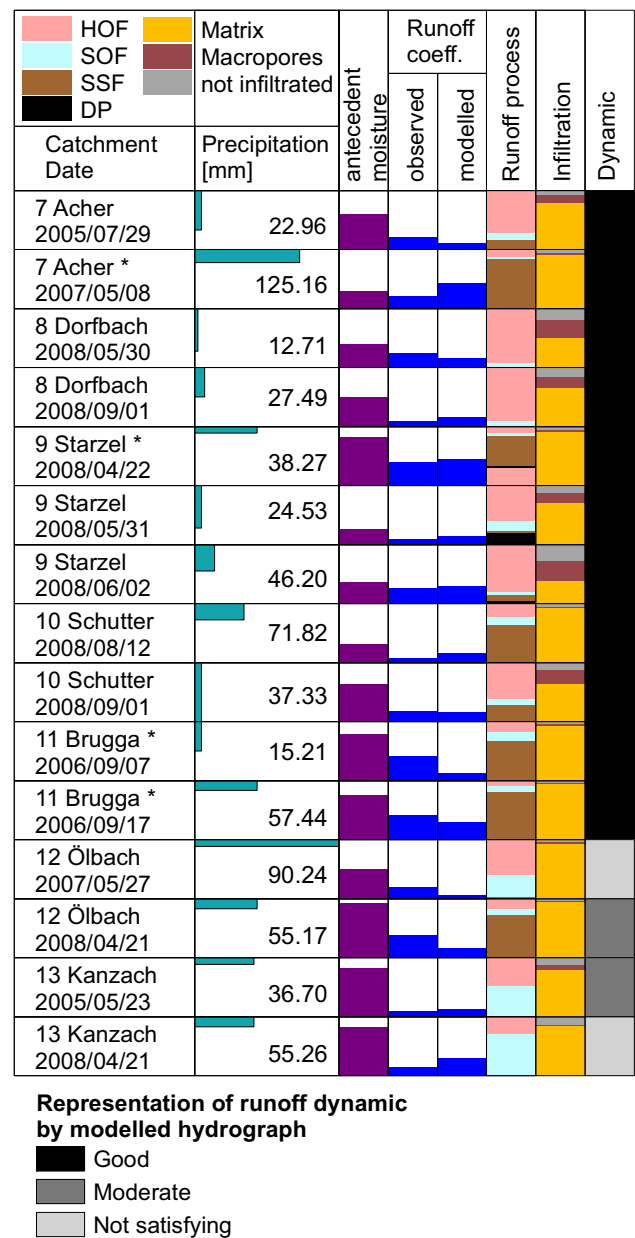


Fig. 8 Overview of event characteristics and model reaction. The area of the precipitation rectangle is proportional to the mean catchment precipitation amount. The width is proportional to event length. Antecedent moisture is the fraction of plant available field capacity filled with water. The percentage of runoff processes (*HOF* Hortonian overland flow, *SOF* saturation overland flow, *SSF* subsurface flow, *DP* deep percolation) is related to the total simulated

characteristics, while Fig. 9 displays the quantitative comparison of the simulation results with observed discharge data at the gauging stations. RoGeR is particularly sensitive to event types and antecedent moisture conditions (Fig. 8). For example, high proportions of SSF occur particularly for long-lasting, advective events and high antecedent moisture conditions. Infiltration processes depend



discharge. Percentage of total infiltration (matrix plus macropores) is related to the amount of precipitation. The grey area in the precipitation column represents the amount of precipitation not infiltrating into the soil. Events, marked by an asterisk, were influenced by measurement problems either of rain radar or discharge. The representation of the dynamic was evaluated subjectively (see text)

mainly on the event type (rainfall intensity) and the soil properties. High proportions of infiltration through macropores are related to convective events in catchments with dominating clay and silt soils. There is a significant disagreement between model and reality for the runoff coefficients of the advective events in catchments no. 3, 4 and 12. The model predicts subsurface runoff as an

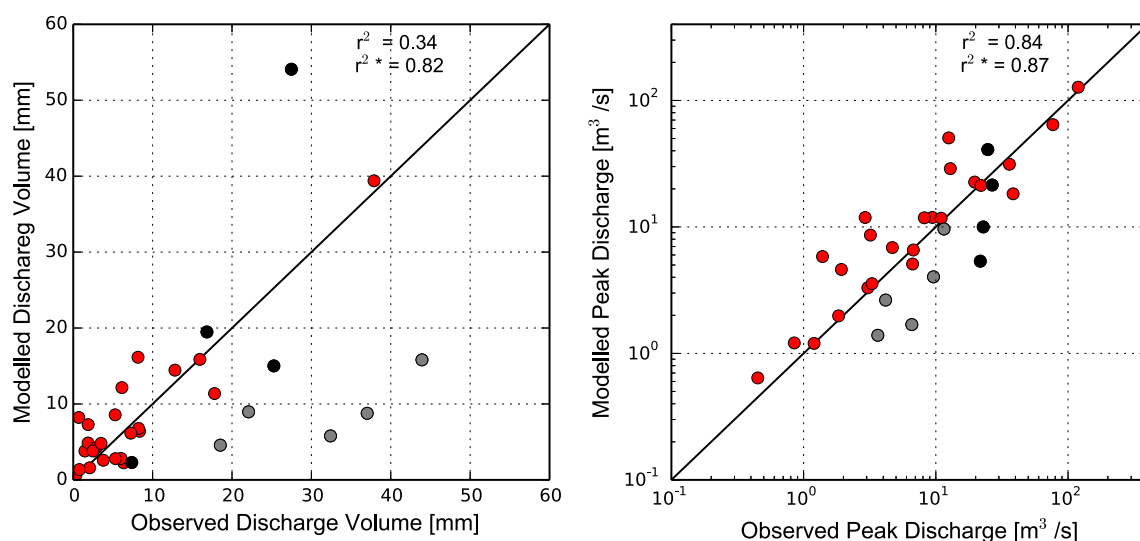


Fig. 9 Simulated versus measured discharge volume and peak discharge of the 33 predicted events of 13 different catchments in BW. The *black dots* represent events during which measurement problems of either rain radar or discharge gauge occurred. For the events represented by *grey dots* (catchments 3, 4 and 12), the

subsurface flow was underestimated presumably by incorrect representation of soil storage capacity, deep percolation or missing data about abundance of periglacial sediment formations. The coefficient of correlations marked by an *asterisk* was calculated without the events marked by *black* and *grey dots*

important runoff component. However, the observed hydrograph shows an even larger proportion of subsurface flow generating the high runoff coefficients. It can be assumed that soil storage capacity and potential deep percolation into the bedrock might not be well represented in those catchments using the available input data. All large deviations between observed and modelled runoff coefficients were either caused by an underestimation of subsurface flow by the model or obvious problems with the observed data (discharge measurements at the gauging sites or the rainfall radar data). The first issues are indicated by the grey colour dots in Fig. 9, and the last by the black colour dots. The underestimation of fast subsurface flow is probably a consequence of missing or incorrect information on the subsurface within the soil and geological data set, for example missing information about periglacial sediment formation, overestimation of soil storage capacity or an overestimation of the deep percolation rate.

The agreement between observed and modelled dynamics of the hydrographs was evaluated and grouped subjectively into three classes: “good”, “moderate” and “not satisfying” (Fig. 8, right column). A good agreement means that shape and quantitative proportion of the simulated runoff components as well as the total flood hydrograph were well suited to reproduce the observed flood hydrographs shape. A moderate agreement means that the shape of the observed hydrograph was well represented by the shape of the simulated runoff components, but the quantity was not well represented. A not satisfying agreement indicates that shape and quantity were not well

reproduced. This subjective approach was selected since all objective functions (e.g. coefficient of correlation, efficiency) are unable to reflect the agreement of the hydrograph shape properly. For example, in Fig. 7 for the long-lasting event in catchment no. 6, the coefficient of correlation is only at 0.56, but the similarity of the modelled versus the observed dynamic is quite satisfying considering the small time lag between simulated and observed peak flow and the shape of the recession. Overall, 21 of 33 events could be modelled with a good agreement of the dynamics between the observed and simulated hydrographs. Five events show a moderate agreement and 7 were not satisfying. Five of the not satisfying results were likely caused by underestimation of subsurface flow. One was caused by an overestimation of SOF, which is quite sensitive to the estimation of the groundwater level (see also discussion above regarding Fig. 7, left bottom). Finally, one event (in catchment 13) was influenced by lake retention, which is not well represented by RoGeR.

One of the main problems of the event-based simulation is the high uncertainty of precipitation and antecedent moisture conditions. The rain radar data are calibrated to precipitation gauging stations and is therefore, for example, affected by shading effects, station density, topographic effects and precipitation type. The antecedent moisture data are itself a model output, which depends on the model structure and input data uncertainty. Taking these input uncertainties into account, the agreement between RoGeR output and observed discharge is satisfying, in particular since the model was not calibrated at all.

Discussion and conclusions

While extensive parameter calibration is still the status quo in rainfall-runoff modelling, RoGeR proved to be a suitable model framework to predict event-based runoff generation processes at the hillslope scale, in headwaters and in mesoscale catchments without any parameter calibration. Taking into account the input uncertainty and the still unresolved problems such as parameterizing macropore properties for a heterogeneous landscape, the results are very satisfying and promising. The application of RoGeR to hillslope sprinkler experiments reproduced the measured overland and subsurface discharge very well. Considering the efforts to simulate these hillslope experiments with numerical 2D Richards-based models (e.g. Faeh et al. 1997), the results show a great potential even at this smaller spatial scale. Larger sets of data from more sprinkler experiments might lead to an even better validation of the model on the one hand. On the other hand, they may also provide crucial information to evaluate if important processes are missing in the model. For example, the development of the model algorithms describing infiltration by shrinkage cracks resulted from poor model prediction in catchments with clayey soils during dry summer months.

There are some other potentially relevant processes like water repellency, soil sealing on silty soils, lake retention, fluctuation of groundwater table or the influence of tile drains. These processes have not yet been implemented into RoGeR because of the lack of data or process understanding. Further progress in deriving geodata can further enhance the ability of RoGeR and reduce uncertainty. The ability of RoGeR to quantify the spatial and temporal distribution and dynamics of runoff generation without parameter calibration makes it a suitable tool for the prediction of flash floods induced by heavy rainfall events at scales up to 10–20 km² where discharge gauging data are lacking. Currently, RoGeR is applied for the whole area of Baden-Württemberg to derive planning criteria for flash flood management based on scenarios of extreme precipitation (LUBW 2016).

A dynamic hydraulic approach for RoGeR is currently still in the developmental stage. It accounts for time variable flow velocities and re-infiltration of overland flow into areas with higher infiltration rates. It might improve the prediction of flow accumulation for small areas and highly intensive rain events. A description of this approach will be subject of a separate publication.

Acknowledgements We thank Simon Scherrer for providing the data of the six hillslope sprinkling experiments. The work was partly funded by the State Office for the Environment, Measurement and Nature Conservation of the Federal State of Baden-Württemberg.

References

- Ad-Hoc-Arbeitsgruppe Boden (2005) *Bodenkundliche Kartieranleitung*. 5. Auflage, Bundesanstalt für Geowissenschaften und Rohstoffe (Hrsg.), Hannover. Schweizerbart, Stuttgart
- Baram S, Kurtzman D, Dahan O (2012) Water percolation through a clayey vadose zone. *J Hydrol* 424–425:165–171
- Berg P, Moseley C, Haerter JO (2013) Strong increase in convective precipitation in response to higher temperatures. *Nat Geosci* 6(3):181–185
- Beven KJ (2011) *Rainfall-runoff modelling: the primer*. Wiley, London
- Beven KJ, Clarke RT (1986) On the variation of infiltration into a homogeneous soil matrix containing a population of macropores. *Water Resour Res* 22(3):383–388
- Bouma J, Dekker LW (1978) A case study on infiltration into dry clay soil. *Geoderma* 20:27–40
- Bremicker M (2000) *Das Wasserhaushaltsmodell LARSIM—Modellgrundlagen und Anwendungsbeispiele* Freiburger Schriften zur Hydrologie, 11, Institute of Hydrology (Hrsg.)
- Casper M (2002) *Die Identifikation hydrologischer Prozesse im Einzugsgebiet des Dürreychbaches (Nordschwarzwald)*. Mitteilungen des Instituts für Wasserwirtschaft und Kulturtechnik der Universität Karlsruhe (TH), Heft 210
- DVWK (1984) *Arbeitsanleitung zur Anwendung von Niederschlag-Abfluß-Modellen in kleinen Einzugsgebieten, Teil II: Synthese, DVWK-Regeln zur Wasserwirtschaft 113*, Deutscher Verband für Wasserwirtschaft und Kulturbau e.V. (DVWK), Bonn
- Faeh AO, Scherrer S, Naef F (1997) A combined field and numerical approach to investigate flow processes in natural macroporous soils under extreme precipitation. *Hydrol Earth Syst Sci* 4:787–800
- Geitner C, Mätzler A, Bou-Vinals A, Meyer E, Tusch M (2014) Bodeneigenschaften und die Besiedlung durch Regenwürmer (Lumbricidae) auf Grünlandstandorten im Brixenbachtal (Kitzbüheler Alpen, Tirol). *Die Bodenkultur* 65(1):39–51
- Green WH, Ampt GA (1911) Studies in soil physics. I The flow of air and water through soils. *J Agric Sci* 4:1–24
- Gudera T, Morhard A (2015) Hoch aufgelöste Modellierung des Bodenwasserhaushalts und der Grundwasserneubildung mit GWN-BW. *Hydrologie und Wasserbewirtschaftung* 59.JahrgangHeft 5:205–216
- Ippisch O, Vogel H-J, Bastian P (2006) Validity limits for the van Genuchten-Mualem model and implications for parameter estimation and numerical simulation. *Adv Water Res* 29(12):1780–1789
- Jarvis NJ, Moeys J, Hollis JM, Reichenberger S, Lindahl AML, Dubus IG (2009) A conceptual model of soil susceptibility to macropore flow. *Vadose Zone J* 8:902–910
- Kohl B, Stepanek L, Pirkl H, Kirnbauer R, Meyer V, Markart G (2012) Verbesserungspotentiale bei der prozessorientierten Ereignismodellierung. *Forum für Hydrologie und Wasserbewirtschaftung* Heft 33(13):147–156
- Konrad JM, Ayad R (1997) Desiccation of a sensitive clay: field experimental observations. *Can Geotech J* 34:929–942
- Li H, Zhang LM (2010) Geometric parameters and REV of a crack network in soil. *Comput Geotech* 37(2010):466–475
- Lindahl AML, Dubus IG, Jarvis NJ (2009) Site classification to predict the abundance of the deep-burrowing earthworm. *Vadose Zone J* 8(2009):911–914
- LUBW Landeanstalt für Umweltschutz Baden-Württemberg (Hrsg.) (1997) *Boden als Lebensraum für Bodenorganismen—bodenbiologische Standortklassifikation—Literaturstudie*, Handbuch Boden

- LUBW Landeanstalt für Umweltschutz Baden-Württemberg (Hrsg.) (2016) Leitfaden Kommunales Starkregenisikomanagement in Baden-Württemberg
- Lutz W (1984) Berechnung von Hochwasserabflüssen unter Anwendung von Gebietskenngrößen. Mitteilung Nr. 24 des Instituts für Hydrologie und Wasserwirtschaft, Universität Karlsruhe
- LUWG, Landesamt für Umwelt, Wasserwirtschaft und Gewerbeaufsicht Rheinland-Pfalz (Hrsg.) (2006) Bestimmungsschlüssel von hochwasserrelevanten Flächen. Bericht Nr. 18
- Markart G, Kohl B, Sotier B, Schauer T, Bunza G und Stern R (2006) Geländeanleitung zur Abschätzung des Oberflächenabflussbeiwertes bei Starkregen—Grundzüge und erste Erfahrungen. Wiener Mitteilungen Band 197: Methoden der hydrologischen Regionalisierung. 159–178
- McGlynn BL, McDonnell JJ, Seibert J, Kendall C (2004) Scale effects on headwater catchment runoff timing, flow sources, and groundwater-streamflow relations. *Wat Resour Res* 40(7):1–14
- Mein RG, Larson CL (1973) Modelling infiltration during a steady rain. *Water Resour Res* 9(2):384–394
- Merz R (2006) Regionalisierung von Ereigniskenngrößen. Wiener Mitteilungen Band 197: Methoden der hydrologischen Regionalisierung. 179–194
- Moldenhauer K-M, Heller K, Chiffard P, Hübner R, Kleber A (2013) Influence of Cover Beds on Slope Hydrology. *Dev Sedimentol* 66:140–152
- Olaya V (2004) A gentle introduction to SAGA GIS. Edition 1.1. The SAGA User Group e.V. (Hrsg.), Göttingen, Germany
- Peschke G (1985) Zur Bildung und Berechnung von Regenabfluss. *Wissensch. Zeitschrift der TU Dresden* Nr. 34(4):195–200
- Pohl B (2000) Charakterisierung der hydrologischen Systemparameter des Einzugsgebietes einer Trinkwasserquelle im Karst am Beispiel Röschenz (Nordwestschweiz), zur differenzierten Ausscheidung von Grundwasserschutzzonen. Diploma thesis at the Institute of Hydrology Freiburg (not published)
- Raissi F, Müller U, Meesenburg H (2009) Ermittlung der effektiven Durchwurzelungstiefe von Forststandorten. *GeoFakten* 9:1–7
- Scherrer S (1997) Abflussbildung bei Starkniederschlägen. Identifikation von Abflussprozessen mittels künstlicher Niederschläge. Mitteilungen der Versuchsanstalt für Wasserbau, Hydrologie und Glaziologie, ETH Zürich, Nr. 147
- Schmocker-Fackel P (2004) A method to delineate runoff processes in a catchment and its implications for runoff simulations. ETH Zürich, Diss
- Schulla J (1997) Hydrologische Modellierung von Flussgebieten zur Abschätzung der Folgen von Klimaänderungen. Diss. 12018, ETH Zürich, 161 S
- Sohrt J, Ries F, Sauter M, Lange J (2014) Significance of preferential flow at the rock soil interface in a semi-arid karst environment. *Catena* 123:1–10
- US-SCS (1972) National engineering handbook section 4 hydrology. US Department of Agriculture
- Van Schaik NLMB (2009) Spatial variability of infiltration patterns related to site characteristics in a semi-arid watershed. *Catena* 78:36–47
- Weiler M (2001) Mechanisms controlling macropore flow during infiltration. Dye tracer experiments and simulations. Schriftenreihe des Instituts für Hydromechanik und Wasserwirtschaft der ETH Zürich, Band 7
- Weiler M (2005) An infiltration model based on flow variability in macropores: development, sensitivity analysis and applications. *J Hydrol* 2005(310):294–315
- Weiler M, Flühler H (2004) Inferring flow types from dye patterns in macroporous soils. *Geoderma* 120(1–2):137–153
- Weiler M, McDonnell J (2004) Virtual experiments: a new approach for improving process conceptualization in hillslope hydrology. *J Hydrol* 285(1):3–18
- Weiler M, Naef F (2003) An experimental tracer study of the role of macropores in infiltration in grassland soils. *Hydrol Process* 17(2):477–493
- Wessolek G, Kaupenjohann M, Renger M (2009) Bodenphysikalische Kennwerte und Berechnungsverfahren für die Praxis. *Bodenökologie und Bodengenese* Heft 40
- Winter F (2013) Prozessorientierte Modellierung der Abflussbildung und -konzentration auf verschlammungsgefährdeten landwirtschaftlichen Nutzflächen. Mitteilungen der Universität der Bundeswehr München, Institut für Wasserwesen Wasserwirtschaft und Ressourcenschutz, Heft 118
- Zillgens B, Merz B, Kimbauer R, Tilch N (2007) Analysis of the runoff response of an alpine catchment at different scales. *Hydrol Earth Syst Sci* 11(4):1441–1454